Letter

Observation of a single quantized vortex vanishment in exciton-polariton superfluids

Daegwang Choi,[1,*] Min Park,[1,*] Byoung Yong Oh,[1] Min-Sik Kwon,[1,2] Suk In Park,[3] Sooseok Kang,[3] Jin Dong Song,[3] Dogyun Ko,[4,5] Meng Sun,[4,†] Ivan G. Savenko,[4,5] Yong-Hoon Cho,[1,2,‡] and Hyoungsoon Choi[1,2,§]

[1]*Department of Physics, Korea Advanced Institute of Science and Technology (KAIST), Daejeon, 34141, Republic of Korea*

[2]*KI for the NanoCentury, Korea Advanced Institute of Science and Technology (KAIST), Daejeon, 34141, Republic of Korea*

[3]*Center for Opto-Electronic Convergence Systems, Korea Institute of Science and Technology (KIST), Seoul, 02792, Republic of Korea*

[4]*Center for Theoretical Physics of Complex Systems, Institute for Basic Science (IBS), Daejeon 34126, Republic of Korea*

[5]*Basic Science Program, Korea University of Science and Technology (UST), Daejeon 34113, Republic of Korea*

(Received 28 September 2020; revised 11 January 2022; accepted 14 January 2022; published 14 February 2022)

We report the direct observation of a single quantized vortex vanishing from a microcavity exciton-polariton superfluid. Exciton-polariton vortices generated by a nonresonant Laguerre-Gaussian optical pumping beam reveal themselves in the energy-integrated emission image, representing a multimode entity consisting of the ground- and excited states. From the time-resolved spectroscopy measurements utilizing various Laguerre-Gaussian beam sizes, we find that the two lowest-energy states get populated and compete with each other, manifested by the change in their mutual population with the beam diameter. Furthermore, we study the transition from the excited state characterized by the finite orbital angular momentum (and a vortex in the direct space) to the ground state under pulsed excitation conditions. Our experimental findings are in excellent agreement with the numerical calculations employing the driven-dissipative Gross-Pitaevskii equation coupled with pumping reservoirs. Thus, our study provides an experimental and theoretical platform to investigate nonequilibrium vortex dynamics and manipulate multistate polariton condensates in semiconductor microcavities.

DOI: 10.1103/PhysRevB.105.L060502

A superfluid is intrinsically different from normal fluids because of its macroscopic quantum coherence. The single valuedness of the wave function, which is used to describe the superfluid state, results in the quantization of circulation in units of $\hbar/m$, where $\hbar$ is the reduced Planck constant, and m the mass of the particle. This quantized circulation in the superfluid carries an integer multiple of 2π phase winding around the vortex core, whose superfluid density is depleted. Since the first prediction by Onsager [1], the generation of quantized vortices has been extensively investigated in conventional single-component bosonic superfluids such as liquid helium [2,3] and cold atomic gases [4,5]. The macroscopic phase winding associated with a quantized vortex makes it a topologically stable object; hence, these vortices can be potentially used as quantized information bits [6]. Their topological stability has drawn attention in terms of particle injection and decay dynamics [7–9].

In most cases, the stability of such topological objects is strongly linked to the stability of the system itself. It is unclear how robust a topological vortex would or should be if an intrinsically dissipative system can form a superfluid. Exciton-polaritons (later *polaritons*) offer a platform for studying the stability of a topological vortex in a nonequilibrium superfluid [10,11]. A polariton is a quasiparticle produced by light-matter interaction between a cavity photon and a quantum-well exciton in a semiconductor microcavity. The excitonic component allows the interaction between polaritons, and the photonic component allows the polaritons to have a short lifetime which leads to the nonequilibrium physics [12,13]. Nevertheless, it is well acknowledged that their bosonic nature allows the formation of macroscopic quantum phenomena such as polariton condensation [14], superfluidity [15], and quantized circulation [16]. In particular, numerous theoretical [17–20] and experimental methods have been developed for creating quantized vortices in polariton systems, including the resonant excitation by Laguerre-Gaussian (LG) beams [21], optical parametric oscillations [22], and circular grating structures [23]. Recently, polariton superfluids have been reported to host quantized vortex states even under nonresonantly pumped LG beam excitation [24].

The combination of nonequilibrium nature of the exciton-polariton condensate and the photonic component that makes imaging of the system readily available creates a unique opportunity for studying the time-resolved dynamics of these vortices. In fact, the creation of multiply charged vortices [25,26] and decay of vortices have been investigated, such as vortex-antivortex pair annihilation [27,28], vortex annihilation through spiraling out of condensates [29], and the destruction of the condensate itself [22]. However, the dynamics associated with vanishment of a single polariton vortex within the polariton condensate lifetime has not been reported.

In this Letter, we report the vanishing of a single quantized vortex in a polariton superfluid. We created a vortex using a *nonresonant* LG beam, which imprints the orbital

*These authors contributed equally to this work.

†Present address: Faculty of Science, Beijing University of Technology, Beijing 100124, China.

‡yhc@kaist.ac.kr

§h.choi@kaist.ac.kr

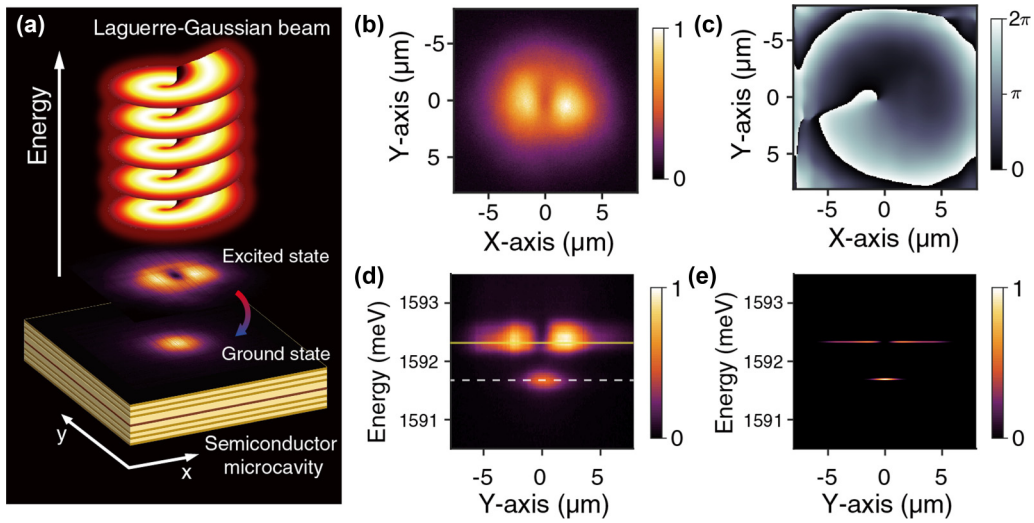

FIG. 1. (a) Schematic illustration of experiment. Semiconductor microcavity is excited by nonresonant LG beam with OAM $|l| = 1$. Above the pumping threshold, polariton condensates are formed in two different energy states with different density distribution. (b) Energy-integrated PL image of the condensates above the threshold density. (c) Phase map of (b) shows 2π phase winding. (d) Real-space spectrum along line $x = 0$ in (b). (e) Calculated real-space spectrum of the condensate.

angular momentum (OAM) of the pump beam to the polariton condensate [24]. The vortex shows an incomplete depletion of the superfluid density at the center when the energy-integrated photoluminescence (PL) image is taken. A careful spectral analysis of this vortex reveals that the polaritons exhibit multimode condensation. We discovered that the incomplete depletion of the superfluid density at the vortex core is an artifact of the time-averaged measurement of the multimode condensate, as evidenced by energy-resolved interferometry experiments. By extracting the phase profile of the wave functions in these two distinct energy states separately, we discovered that only the excited state carries an angular momentum, and hence, a quantum vortex. Furthermore, time-resolved spectroscopy shows that relaxation occurs from the excited (vortex) state to the stationary ground state in a pulsed LG beam, which serves as a direct experimental signature of a quantized vortex vanishing from the system. Such a transition is manifested by changing the size of the LG beam. Using continuous-wave (cw) excitation, we can achieve a steady state, in which the excited- and ground states coexist.

Our observations are supported by a theoretical model based on the driven-dissipative Gross-Pitaevskii equation coupled with incoherent and coherent reservoirs; hence, we suggest a mechanism for OAM transfer from the pump beam to the polariton condensate that is based on the microscopic coherent properties of the latter. Furthermore, we explain the transition of the system from the first excited state characterized by the vortex and a concrete OAM to the intermediate regime, when two lowest-energy states coexist, and finally, to the ground-state condensate with zero OAM after the vortex vanishes.

The experiment was performed for a GaAs quantum well (QW) microcavity using the nonresonant excitation with an LG beam, as depicted in Fig. 1(a). A pair of distributed Bragg reflectors forms an optical cavity of $\lambda/2$ with a set of GaAs/AlAs QW stacks (for details, see the Supplemental Material [30]). The sample was placed inside a cryostat (with an optical window) reaching as low as 5 K. A pulsed and a cw excitation by a Ti:sapphire laser with an energy of 1.72 eV (720 nm), which is considerably higher than the QW band gap, were used to nonresonantly pump electron-hole plasma into the QWs. An LG beam was generated as the Gaussian laser beam passed a 2π winding phase mask, which resulted in an OAM of the $l = +1$ beam [Fig. 2(a)]. Above the threshold density, polaritons formed condensates with a quantized vortex. We measured the energy-integrated PL image [Fig. 1(b)] and phase map [Fig. 1(c)] under pulsed excitation. The fact that 2π phase winding is measured in the phase map implies that the superfluid carries a circulation of $\hbar/m$. However, the real-space spectrum along $x = 0$ [Fig. 1(d)] clearly shows that the condensate is not in a static uniform state but two quantized states. For simplicity, the higher- and lower-energy states will be referred to as the excited and ground states, respectively. For the theoretical description of the experiment, we used a driven-dissipative Gross-Pitaevskii equation coupled with incoherent and coherent reservoirs, where the latter carries the same OAM as the LG beam (see Ref. [30] for the details of the model). We assume that the OAM of the pumping source is almost erased in the scattering processes, and only a small amount of it remains. The OAM is revived in the polariton condensate owing to the interaction with a weak coherent reservoir and the coherent properties of the condensate. Figure 1(e) exhibits a simulation result of multistate condensate similar to that in the experiment.

To investigate the density distribution and phase information in each state, we employed energy-resolved spatial interferometry based on the tomographic measurement protocol [31–35]. The experimental procedure was similar to the modified Mach-Zehnder interferometry, which is typically used to visualize quantized vortices [10,24]. To represent energy-resolved data, we selected $E = 1592.37$ meV for the excited state and $E = 1591.69$ meV for the ground state, which are denoted in Fig. 1(d) as yellow solid and white dotted lines, respectively. Figures 2(b) and 2(c) show the

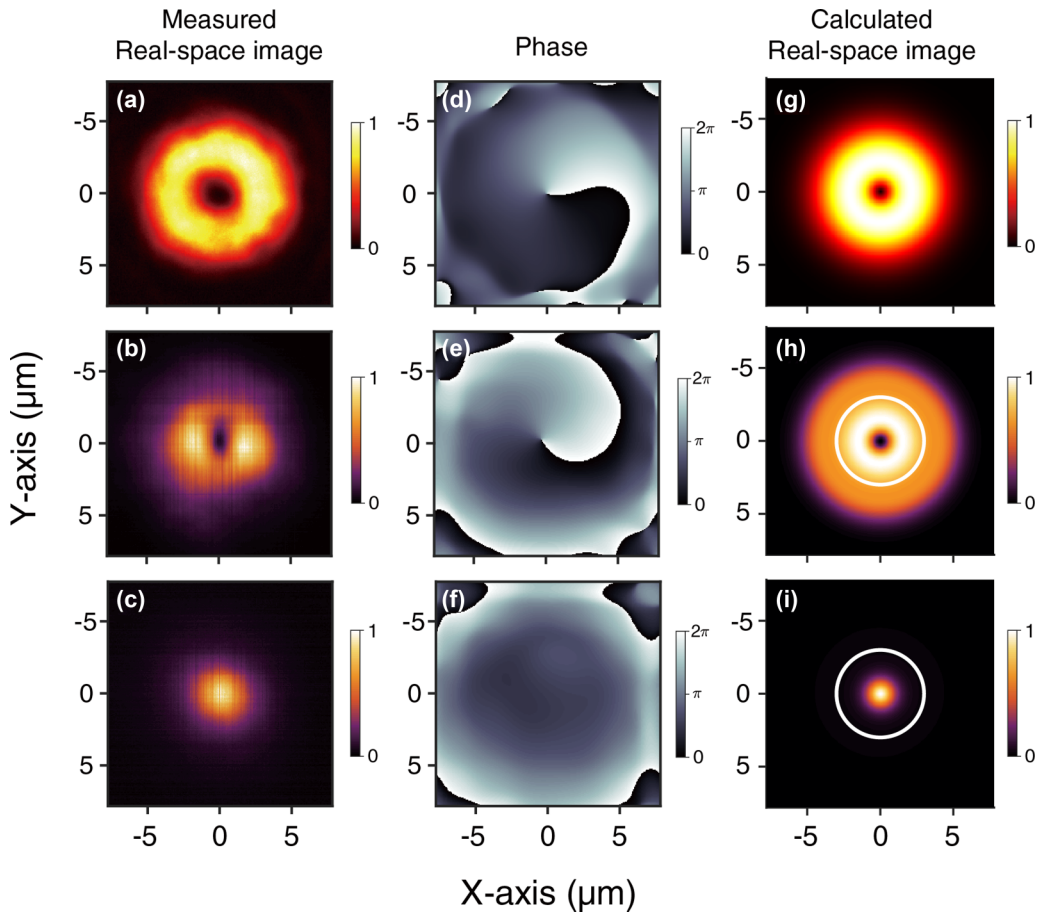

FIG. 2. Pump and condensates profiles. (a) LG pump intensity distribution; energy-resolved PL images of (b) excited state at 1592.37 meV, and (c) ground state at 1591.69 meV under pulsed excitation; (d) phase map of LG beam having OAM $l = +1$; phase maps of (e) excited state and (f) ground state. A 2π phase winding in (e) indicates quantized vortex in excited state. Panels (g), (h), and (i) show calculated real-space images of LG beam excitation and polariton condensates, when the system is stationary (either ground or excited state). White circles in panels (h) and (i) indicate nominal diameter (6.0 μm) of LG beam corresponding to maximum intensity spots of simulated beam (g).

energy-resolved PL intensity images under pulsed excitation, which represent the spatial polariton densities at the excited- and ground energy levels, respectively. As shown in Fig. 2(b), the density minimum in the center is clearly observed in the excited state, whereas the ground state exhibited a Gaussian density distribution [Fig. 2(c)]. The phase maps retrieved from the interference patterns of these two states are shown in Figs. 2(e) and 2(f). The excited state shows a clear 2π phase winding with respect to the density minimum point, indicating a quantized vortex. The phase winding of the vortex [Fig. 2(e)] was identical to the OAM of the LG pump [Fig. 2(d)]. However, the phase map for the ground state indicated no such phase winding, and the phase was relatively flat aside from the radial gradient [Fig. 2(f)]. In other words, the ground state did not carry any vortices.

The simulated LG beam [Fig. 2(g)] resulted in polariton condensate formation at the two energy levels [Fig. 1(e)]. The real-space emission profiles in the steady state for each of these energy levels are shown in Figs. 2(h) and 2(i), exhibiting consistency with the experiment. (To simulate the formation of the ground- and excited states, we used the cw excitation instead of the exact femtosecond-order pulsed excitation [30]).

The time-integrated real-space spectra measurement shows that the relative intensity of the PL emission from the two states depends on the diameter of the LG beam, as shown in Fig. 3(a). For a beam with a smaller diameter (4.5 μm or less), only the ground state is populated. However, as the beam diameter increases, the intensity of the excited-state emission increases, and at a sufficiently large diameter, the ground state becomes almost invisible. This can be understood as a confinement effect: the excited state is being pushed out of the potential trap if the beam spot is sufficiently small. As the beam diameter increases, the spatial confinement reduces, resulting in a redshift [Fig. 3(b)]. Once the first excited-state energy becomes sufficiently low and fits inside the potential trap, the condensate forms in the excited state. This behavior was confirmed via numerical calculations. Both the experimental results and the numerical calculations are depicted in Fig. 3(b). The figure shows energy of the ground state and the excited state for different beam diameters. The data slope downwards as the beam diameter increases due to the reduced blueshift with smaller confinement.

The time-integrated measurement is not suitable for determining the exact nature of the multistate condensate under the pulsed excitation because it does not allow us to understand

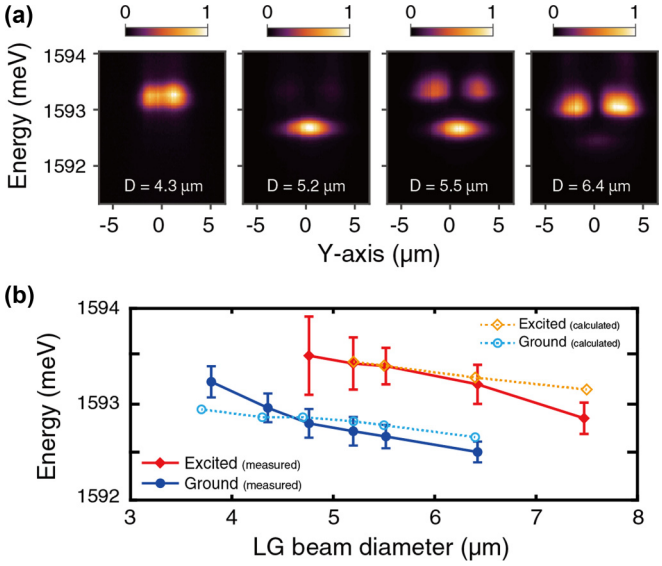

FIG. 3. (a) Real-space spectra of PL profiles in pulsed-excitation regime for different pumping beam diameters of 4.3, 5.2, 5.5, and 6.4 μm. Beam diameter is defined as distance between two maxima of laser profile [Fig. 2(a)]. (b) Energy of ground- (blue circle) and first excited (red diamond) states as a function of beam diameter. The numerical simulation of ground- (open circle) and excited states (open diamond) are plotted.

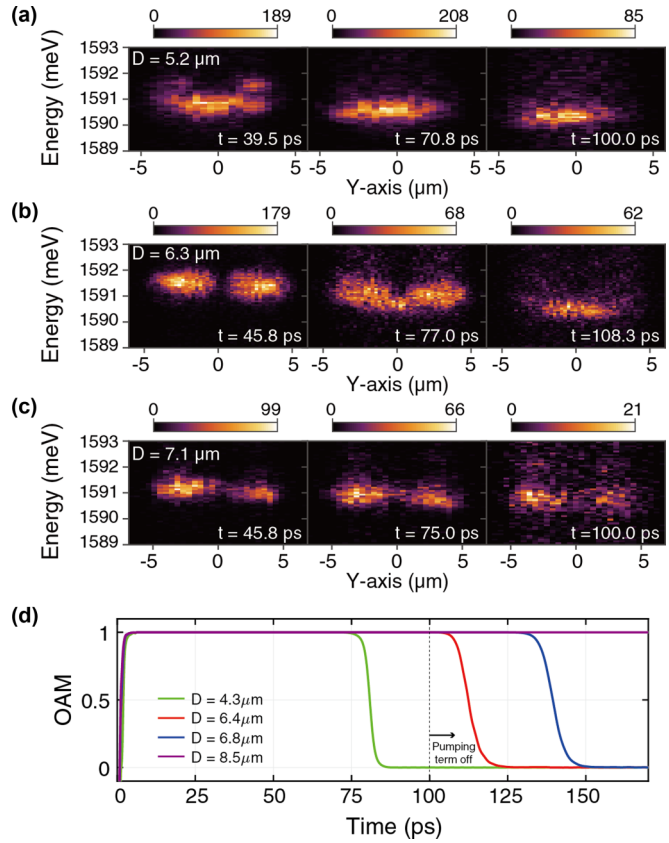

FIG. 4. Time-resolved spectroscopy of polariton vortex in pulsed LG pump regime for different beam radii: (a) 5.2, (b) 6.3, and (c) 7.1 μm. Data were measured along straight line through center of beam (at $x = 0\,\mu$m). (d) Simulation of OAM evolution for different beam diameters with same initial condition. To simulate the pulsed excitation case, the pumping term was turned off after 100 ps.

whether polaritons occupy the two lowest-energy states simultaneously or sequentially. To distinguish between these two possible scenarios, we performed time-resolved real-space spectroscopy, allowing us to measure the relative intensity of the two states and directly relate it to particular time intervals [Figs. 4(a)–4(c)]. We discovered that the two states appeared sequentially, beginning from the vortex-carrying excited state. Eventually, the system experienced a transition to the ground state. Note, that in a smaller LG beam diameter [Fig. 4(a)], polaritons occupy the "Gaussian" ground state dominantly (appearing as single lobe along the y axis at $x = 0$) in the measured time evolution. However, in the case of intermediate LG beam diameter [Fig. 4(b)], polaritons occupy the "annular" excited state (appearing as double lobes along the y axis at $x = 0$) initially, and they experience a transition to the ground state as time proceeds. In the case of a larger LG beam diameter [Fig. 4(c)], polaritons show only the excited state over the whole time duration. These measurements were also confirmed by simulations (see Ref. [30] and the discussion below). Our simulations indicate that the transition phenomena were accompanied by the competition between two energy states as well as the lowering of the potential barrier [36] as time proceeds under the pulsed excitation. In fact, the transition to the lower-energy state occurred due to scattering processes [37]. When the population of the ground state increases, polaritons try to occupy the *center* of the potential trap, where the vortex core is located. Hence, the growing ground state competes with the excited state for the central location and attempts to push the excited state out from the interior of the LG beam area. In pulsed excitation, the gradual depletion of the exciton reservoir over time results in a reduction in the potential barrier (as compared with cw excitation). Then, the excited state is pushed out faster, and the system remains in the ground state. For sufficiently large beam diameters [e.g., Fig. 4(c)], the entire process can take longer than the condensate lifetime, and polaritons decay before the transition occurs. For smaller beam diameters [e.g., Fig. 4(a)], the excited state can be pushed out more easily; hence, an earlier transition to the ground state can be observed. Although the total OAM of the polaritons will not reach complete unity in practice because of inherent fluctuations in the sample and the nonideality of the LG beam, the simulation explains well what we see in the experiments [Fig. 4(d)]: a smaller beam size resulted in the sooner loss of the total OAM of the system. We investigated the dependence of the OAM on the size of the LG beam and its intensity in the regime of the pulsed exaction. Detailed model and the theoretical methods are described in Supplemental Material [30].

In our observations, the OAMs of the initial and final states were different. A quantized vortex vanishes in the transition to ground state. There have been previous reports on the decay of vortices in polariton superfluids, mostly under net angular-momentum conserving conditions, including the most recent experiment [38], which showed that the vortices with OAM $l = +1$ and $l = -1$ can be simultaneously observed, followed by the system decaying to a purely

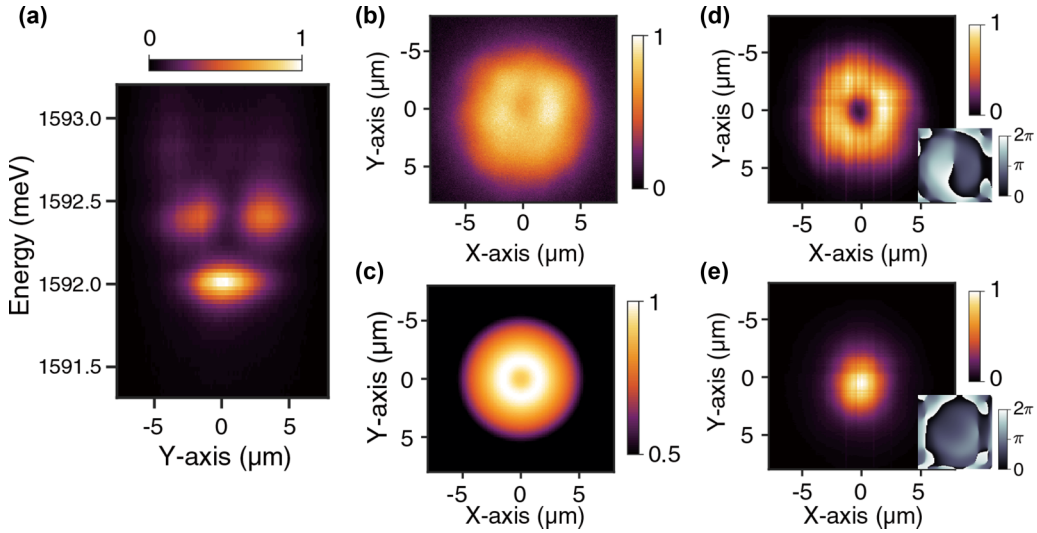

FIG. 5. Steady state of partially rotating polariton superfluid under cw LG beam excitation. (a) Real-space spectrum of polariton condensates. (b) Energy-integrated PL image of system. (c) Calculated polariton distribution [simulation of (b)]. Energy-resolved PL images of excited- and ground states shown in panels (d) and (e), respectively; insets show corresponding phase maps.

zero-OAM ground state under the excitation of $l = 0$ ring-shaped pumping. This is in contrast to our observation, where a single quantized vortex with a net OAM is spontaneously relaxed in an angular-momentum-*nonconserving* manner under an intentional excitation of the $|l| = 1$ LG beam. One of the reasons why we can observe this transition is that we created a single vortex through *nonresonant* excitation. A polariton vortex produced by a resonant excitation would not allow such a transition because it cannot effectively produce a spatial potential from the exciton reservoir [21]. Unlike the vortices in an equilibrium superfluid (which do not evaporate over time), the vortices in polariton condensates might decay if the vortex escapes from the system [29]. We observed the vanishment of the vortex based on time-resolved measurements of the energy-state transition, which cannot be treated as a direct observation of an escaping vortex. We considered this scenario as a distinct possibility, as revealed by our simulations, which show the disappearance of the singularity from the center of the trap. Regardless of the actual mechanism through which the vortex escapes from the system, our experiment presents a knob with which one can control the timing of the switch between the polariton condensates with and without a quantized vortex.

For comparison, we created and investigated a polariton vortex under a cw excitation (not pulsed) in an identical experimental setup and generated $l = -1$ OAM beams; subsequently, we observed two lowest-energy states [Fig. 5(a)]. As shown in Figs. 5(b) and 5(c), the energy-integrated PL image of the system was consistent with the theoretical simulations. The energy-resolved PL images of the excited- and ground states in the cw excitation regime are shown in Figs. 5(d) and 5(e), respectively, with the corresponding phase profiles for each state shown in the insets. One key difference from the pulsed excitation regime is that the cw pump beam permanently supplies the potential barrier, which prevents the excited state from being pushed out easily. The competition between these two energy states alone may not be enough to push the excited state out without the lowering effect of potential barrier during time evolution. Therefore, there is a balance among the pump, decay, and interstate transition processes to maintain a steady state. We emphasize that this steady state represents an intriguing regime in which a vortex-carrying state and a ground state coexist.

In conclusion, using time-resolved spectroscopy, we explicitly demonstrated a single quantum vortex vanishing in an exciton-polariton superfluid pumped by a pulsed nonresonant LG beam. By varying the LG beam size, we investigated the competition between the ground- and first excited states, which determines the population of the multistate condensate and affects the transition between the two states under pulsed excitation conditions. Our experimental findings are consistent with the numerical calculations using the driven-dissipative Gross-Pitaevskii equation coupled with incoherent and coherent reservoirs. The coherent reservoir served as a minute seed (initial condition), resulting in the breaking of the rotational symmetry and the revival of the OAM of the nonresonant excitation with the subsequent formation of a quantum vortex with a predefined winding number. We proposed experimental and theoretical tools to manipulate multistate polariton condensates via potential landscape engineering in semiconductor microcavities; these tools have broad implications in terms of studying light-matter interaction and stability of topological objects in semiconducting devices, and developing polariton devices for quantum communications in the near future.

We would like to thank Prof. Su-Hyun Gong (Korea University, Seoul, Republic of Korea) for the helpful discussions. We acknowledge support from the National Research Foundation (NRF) of Korea through Projects No. NRF-2020M3E4A1080112, No. NRF-2016R1A5A1008184, and No. NRF-2019R1A2C2011538. S.I.P., S.K., and J.D.S. ac-

knowledge the support of the IITP grant funded by the Korea government (MSIT) (Grant No. 20190004340011001) and the KIST institutional program of flagship. D.K., M.S., and I.G.S. acknowledge the support from the Institute for Basic Science in Korea (Project No. IBS-R024-D1).

D.C. and M.P. performed the experiments and analyzed the data. B.Y.O. and M.-S.K. contributed to the experiments at the early stage. The sample was grown by S.I.P., S.K., and J.D.S. Theoretical modeling and calculations were performed by D.K. and M.S. under the supervision of I.G.S. Y.-H.C., and H.C. conceived the project and supervised its development. All authors discussed the results and contributed to the writing of the manuscript.

[1] L. Onsager, Nuovo Cimento **6**, 279 (1949).
[2] E. J. Yarmchuk, M. J. V. Gordon, and R. E. Packard, Phys. Rev. Lett. **43**, 214 (1979).
[3] Y. P. Sachkou, C. G. Baker, G. I. Harris, O. R. Stockdale, S. Forstner, M. T. Reeves, X. He, D. L. McAuslan, A. S. Bradley, and M. J. Davis, Science **366**, 1480 (2019).
[4] M. R. Matthews, B. P. Anderson, P. C. Haljan, D. S. Hall, C. E. Wieman, and E. A. Cornell, Phys. Rev. Lett. **83**, 2498 (1999).
[5] J. Abo-Shaeer, C. Raman, J. Vogels, and W. Ketterle, Science **292**, 476 (2001).
[6] T. Golod, A. Iovan, and V. M. J. N. c. Krasnov, Nat. Commun. **6**, 8628 (2015).
[7] V. M. Ruutu, J. J. Ruohio, M. Krusius, B. Plaçais, E. B. Sonin, and W. Xu, Phys. Rev. B **56**, 14089 (1997).
[8] P. W. Adams and W. I. Glaberson, Phys. Rev. B **35**, 4633 (1987).
[9] V. Bretin, P. Rosenbusch, and J. Dalibard, J. Opt. B: Quantum Semiclassical Opt. **5**, S23 (2003).
[10] K. G. Lagoudakis, M. Wouters, M. Richard, A. Baas, I. Carusotto, R. André, L. S. Dang, and B. Deveaud-Plédran, Nat. Phys. **4**, 706 (2008).
[11] K. Lagoudakis, T. Ostatnický, A. Kavokin, Y. G. Rubo, R. André, and B. Deveaud-Plédran, Science **326**, 974 (2009).
[12] M. H. Szymanska, J. Keeling, and P. B. Littlewood, Phys. Rev. Lett. **96**, 230602 (2006).
[13] M. Wouters and I. Carusotto, Phys. Rev. Lett. **99**, 140402 (2007).
[14] J. Kasprzak, M. Richard, S. Kundermann, A. Baas, P. Jeambrun, J. M. Keeling, F. M. Marchetti, M. H. Szymanska, R. Andre, J. L. Staehli, V. Savona, P. B. Littlewood, B. Deveaud, and L. S. Dang, Nature (London) **443**, 409 (2006).
[15] A. Amo, J. Lefrère, S. Pigeon, C. Adrados, C. Ciuti, I. Carusotto, R. Houdré, E. Giacobino, and A. Bramati, Nat. Phys. **5**, 805 (2009).
[16] G. Liu, D. W. Snoke, A. Daley, L. N. Pfeiffer, and K. West, Proc. Natl. Acad. Sci. **112**, 2676 (2015).
[17] T. C. H. Liew, A. V. Kavokin, and I. A. Shelykh, Phys. Rev. B **75**, 241301(R) (2007).
[18] X. Ma and S. Schumacher, Phys. Rev. Lett. **121**, 227404 (2018).
[19] A. V. Yulin, A. S. Desyatnikov, and E. A. Ostrovskaya, Phys. Rev. B **94**, 134310 (2016).
[20] E. A. Ostrovskaya, J. Abdullaev, A. S. Desyatnikov, M. D. Fraser, and Y. S. Kivshar, Phys. Rev. A **86**, 013636 (2012).
[21] T. Boulier, H. Tercas, D. D. Solnyshkov, Q. Glorieux, E. Giacobino, G. Malpuech, and A. Bramati, Sci. Rep. **5**, 9230 (2015).
[22] D. Sanvitto, F. M. Marchetti, M. H. Szymanska, G. Tosi, M. Baudisch, F. P. Laussy, D. N. Krizhanovskii, M. S. Skolnick, L. Marrucci, A. Lemaitre, J. Bloch, C. Tejedor, and L. Vina, Nat. Phys. **6**, 527 (2010).
[23] J. Hu, S. Kim, C. Schneider, S. Höfling, and H. Deng, Phys. Rev. Appl. **14**, 044001 (2020) .
[24] M.-S. Kwon, B. Y. Oh, S.-H. Gong, J.-H. Kim, H. K. Kang, S. Kang, J. D. Song, H. Choi, and Y.-H. Cho, Phys. Rev. Lett. **122**, 045302 (2019).
[25] S. N. Alperin and N. G. Berloff, Optica **8**, 301 (2021).
[26] T. Cookson, K. Kalinin, H. Sigurdsson, J. D. Topfer, S. Alyatkin, M. Silva, W. Langbein, N. G. Berloff, and P. G. Lagoudakis, Nat. Commun. **12**, 2120 (2021).
[27] E. Cancellieri, T. Boulier, R. Hivet, D. Ballarini, D. Sanvitto, M. H. Szymanska, C. Ciuti, E. Giacobino, and A. Bramati, Phys. Rev. B **90**, 214518 (2014).
[28] R. Hivet, E. Cancellieri, T. Boulier, D. Ballarini, D. Sanvitto, F. M. Marchetti, M. H. Szymanska, C. Ciuti, E. Giacobino, and A. Bramati, Phys. Rev. B **89**, 134501 (2014).
[29] M. Wouters and V. Savona, Phys. Rev. B **81**, 054508 (2010).
[30] See Supplemental Material at http://link.aps.org/supplemental/10.1103/PhysRevB.105.L060502 for experimental setup details and descriptions of theoretical model.
[31] G. Nardin, K. G. Lagoudakis, B. Pietka, F. Morier-Genoud, Y. Léger, and B. Deveaud-Plédran, Phys. Rev. B **82**, 073303 (2010).
[32] G. Nardin, Y. Léger, B. Pietka, F. Morier-Genoud, and B. Deveaud-Plédran, Phys. Rev. B **82**, 045304 (2010).
[33] R. Cerna, D. Sarchi, T. K. Paraïso, G. Nardin, Y. Léger, M. Richard, B. Pietka, O. El Daif, F. Morier-Genoud, V. Savona, M. T. Portella-Oberli, and B. Deveaud-Plédran, Phys. Rev. B **80**, 121309(R) (2009).
[34] V. G. Sala, D. D. Solnyshkov, I. Carusotto, T. Jacqmin, A. Lemaître, H. Terças, A. Nalitov, M. Abbarchi, E. Galopin, I. Sagnes, J. Bloch, G. Malpuech, and A. Amo, Phys. Rev. X **5**, 011034 (2015).
[35] J. V. T. Buller, E. A. Cerda-Méndez, R. E. Balderas-Navarro, K. Biermann, and P. V. Santos, New J. Phys. **18**, 073002 (2016).
[36] A. Askitopoulos, T. C. H. Liew, H. Ohadi, Z. Hatzopoulos, P. G. Savvidis, and P. G. Lagoudakis, Phys. Rev. B **92**, 035305 (2015).
[37] M. Wouters, T. C. H. Liew, and V. Savona, Phys. Rev. B **82**, 245315 (2010).
[38] B. Berger, D. Schmidt, X. Ma, S. Schumacher, C. Schneider, S. Höfling, and M. Aßmann, Phys. Rev. B **101**, 245309 (2020).